Title

Molecular basis of chromatin remodeling by Rhp26, a yeast CSB ortholog.

Journal

Proceedings of the National Academy of Sciences of USA, 116(13)

Authors

Wang, Wei
Xu, Jun
Limbo, Oliver
et al.

Publication Date

2019-03-26

DOI

10.1073/pnas.1818163116

Peer reviewed

Molecular basis of chromatin remodeling by Rhp26, a yeast CSB ortholog

Wei Wang[a,b,c,1], Jun Xu[a,b,1], Oliver Limbo[d,1], Jia Fei[e,1], George A. Kassavetis[e], Jenny Chong[a,b], James T. Kadonaga[e], Paul Russell[d], Bing Li[f,2], and Dong Wang[a,b,2]

[a]Division of Pharmaceutical Sciences, Skaggs School of Pharmacy & Pharmaceutical Sciences, University of California, San Diego, La Jolla, CA 92093; [b]Department of Cellular & Molecular Medicine, School of Medicine, University of California, San Diego, La Jolla, CA 92093; [c]Advanced Medical Research Institute, Shandong University, 250012 Jinan, China; [d]Department of Molecular Medicine, The Scripps Research Institute, La Jolla, CA 92037; [e]Section of Molecular Biology, University of California, San Diego, La Jolla, CA 92093; and [f]Department of Biochemistry and Molecular Cell Biology, Shanghai Key Laboratory for Tumor Microenvironment and Inflammation, Shanghai Jiao Tong University School of Medicine, 200025 Shanghai, China

Edited by Philip C. Hanawalt, Stanford University, Stanford, CA, and approved February 11, 2019 (received for review October 22, 2018)

CSB/ERCC6 belongs to an orphan subfamily of SWI2/SNF2-related chromatin remodelers and plays crucial roles in gene expression, DNA damage repair, and the maintenance of genome integrity. The molecular basis of chromatin remodeling by Cockayne syndrome B protein (CSB) is not well understood. Here we investigate the molecular mechanism of chromatin remodeling by Rhp26, a *Schizosaccharomyces pombe* CSB ortholog. The molecular basis of chromatin remodeling and nucleosomal epitope recognition by Rhp26 is distinct from that of canonical chromatin remodelers, such as imitation switch protein (ISWI). We reveal that the remodeling activities are bidirectionally regulated by CSB-specific motifs: the N-terminal leucine-latch motif and the C-terminal coupling motif. Rhp26 remodeling activities depend mainly on H4 tails and to a lesser extent on H3 tails, but not on H2A and H2B tails. Rhp26 promotes the disruption of histone cores and the release of free DNA. Finally, we dissected the distinct contributions of two Rhp26 C-terminal regions to chromatin remodeling and DNA damage repair.

chromatin remodeling | histone tail | SNF2-like family ATPase | Cockayne syndrome B | nucleosome sliding and eviction

Eukaryotic chromatin-remodeling factors can greatly facilitate the structural rearrangement of the chromatin in an ATP-dependent manner and permit the access of protein factors to execute DNA replication, transcription, recombination, and/or repair (1–5). These enzymes are broadly conserved, and all share a common core ATPase domain with two RecA-like lobes. They can be further divided into four canonical subfamilies based on phylogenetic and functional analyses: imitation switch protein (ISWI), chromodomain helicase DNA-binding protein (CHD), switch/sucrose nonfermentable protein (SWI/SNF), and INO80 (1–5). The mode of remodeling action varies significantly between different subfamily remodelers (5–7). ISWI and CHD subfamily remodelers are involved in nucleosome deposition and spacing mainly by nucleosome sliding, whereas SWI/SNF subfamily proteins can alter the chromatin by repositioning nucleosome and evicting histone octamers or dimers. The INO80 subfamily can promote histone exchange (5).

While the core ATPase provides the driving force for DNA translocation and chromatin-remodeling activity by ATP hydrolysis (3), different flanking domains adjacent to the core ATPase domain play key roles in regulating core ATPase activities, mediating specific recognition with different types of nucleosome substrates or other protein partners and dictating distinct outcomes (such as nucleosome assembly, nucleosome disassembly, and/or specific histone replacement) (1–5). The regulatory mechanism can be remodeler-specific. Taking ISWI as an example, it is inhibited by its AutoN and NegC auto-inhibitory motifs. Binding to the basic patch of H4 tail (R17–R19) releases the inhibition of AutoN motif, whereas binding to the linker DNA through its HAND-SANT-SLIDE (HSS) domain releases NegC inhibition. These ISWI-specific interactions and regulations are not conserved in SWI/SNF remodelers.

Cockayne syndrome group B protein (CSB/ERCC6) has been identified as a member of a distant subfamily of SNF2-like helicases and does not belong to any of the above-mentioned four canonical subfamilies (Fig. 1*A*) (8). CSB/ERCC6 is a key enzyme involved in various cellular processes, such as DNA repair, transcription regulation, and chromatin maintenance (9–13). In particular, CSB/ERCC6 plays an important role in transcription-coupled nucleotide excision repair (TC-NER). It binds the RNA polymerase II (Pol II) stalled complex at DNA damage sites and recruits downstream repair factors (such as CSA/ERCC8, TFIIH, XPA, and UVSSA) to repair DNA damage in the transcribed region (14–18). Mutations of the CSB/ERCC6 gene in humans lead to Cockayne syndrome, a rare neurological disorder that is characterized by premature aging, growth failure, and photosensitivity (10, 14, 19, 20). CSB/ERCC6 proteins are highly conserved in most eukaryotic species (21), including Rad26 and Rhp26 in *Saccharomyces cerevisiae* and *Schizosaccharomyces pombe*, respectively (22–24). CSB proteins can be divided into three regions: the N-terminal region (NTR), the core ATPase domain, and the C-terminal region (CTR). The core ATPase domain is composed of two RecA-like lobes (lobe 1 and lobe 2) containing seven hallmark motifs (I, Ia, II, III, IV, V, and VI) conserved in superfamily helicase 2 (SF2) family proteins (1, 25). We previously

Significance

Cockayne syndrome B protein (CSB), conserved from yeast to humans, plays crucial roles in DNA repair, gene expression, chromatin remodeling, and maintenance. However, the molecular basis of chromatin remodeling by CSB is not well understood. Here we used Rhp26, a yeast CSB ortholog, as a model protein. We revealed that the molecular basis of chromatin remodeling and nucleosomal epitope recognition by Rhp26 is distinct from that of canonical chromatin remodelers. The remodeling activities are bidirectionally regulated by two CSB-specific motifs and depend on H4 tails. This study provides important insights into understanding the molecular mechanisms of chromatin remodeling by CSB and its implications in DNA repair and transcription.

Author contributions: W.W., J.X., O.L., J.F., and D.W. designed research; W.W., J.X., O.L., J.F., J.C., and D.W. performed research; G.A.K., J.C., and B.L. contributed new reagents/analytic tools; W.W., J.X., O.L., J.F., J.T.K., P.R., B.L., and D.W. analyzed data; and W.W., J.X., O.L., J.F., J.C., J.T.K., P.R., B.L., and D.W. wrote the paper.

The authors declare no conflict of interest.

This article is a PNAS Direct Submission.

[1]W.W., J.X., O.L., and J.F. contributed equally to this work.

[2]To whom correspondence may be addressed. Email: bingli@shsmu.edu.cn or dongwang@ucsd.edu.

This article contains supporting information online at www.pnas.org/lookup/suppl/doi:10.1073/pnas.1818163116/-/DCSupplemental.

Published online March 13, 2019.

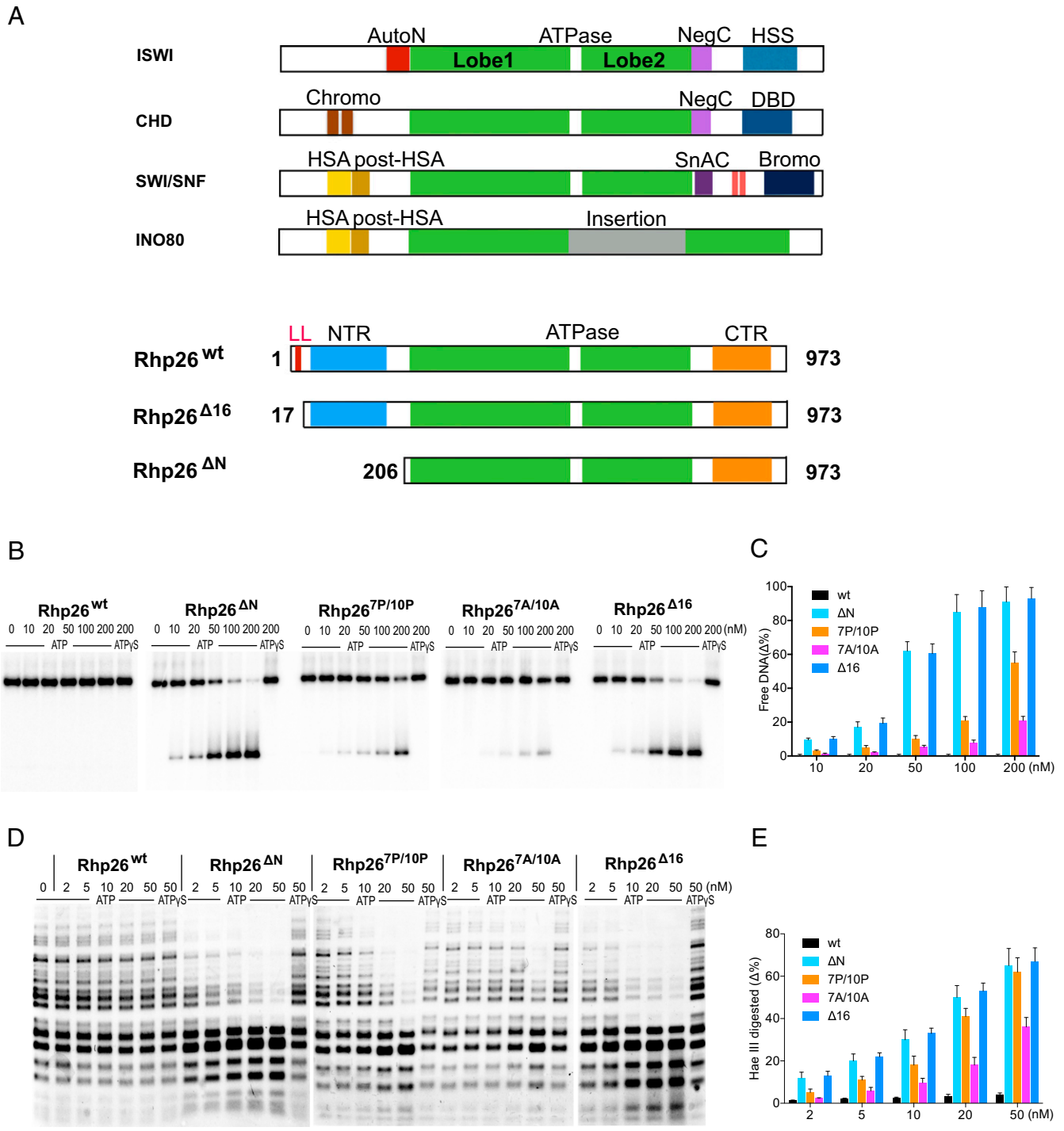

Fig. 1. The orphan remodeler Rhp26/CSB is auto-inhibited by its leucine-latch motif. (*A*) The orphan remodeler CSB is distinct from four canonical subfamilies of SNF2-like remodelers (specific domains are shown in different colors). Schematic diagram of the *S. pombe* CSB ortholog Rhp26 and truncations used in this study. The NTR, core ATPase domain (lobe 1 and lobe 2), and CTR are shown in cyan, green, and orange, respectively. The leucine-latch motif is described as "LL" in red. Other specific domains of four canonical remodelers in abbreviations are listed as below: AutoN, autoinhibitory N-terminal; DBD, DNA-binding domain; HSA, helicase/SANT-associated; HSS, HAND-SANT-SLIDE; NegC, negative regulator of coupling; SnAC, Snf2 ATP coupling. Chromo and Bromo domains recognize methylated and acetylated lysine, respectively. (*B* and *C*) The mutation or deletion of the leucine-latch motif reveals robust remodeling activities using a mononucleosome-remodeling assay. No nucleosome-remodeling activity was observed for Rhp26^{wt}. The 25-nM nucleosome substrate (0-*N*-70) and different concentrations of remodelers were incubated for 1 h at 23 °C before the reaction was quenched. (*D* and *E*) Chromatin-remodeling assay using a circular plasmid template. The final concentration of nucleosomes was 50 nM, and concentrations of remodelers are shown on the top of the gels. The reactions were performed at 23 °C for 1 h. Similar results were obtained in comparison with the mononucleosome-remodeling assay (*B*). All data are displayed as mean and SD ($n = 3$).

identified a conserved leucine-latch motif that plays important auto-inhibitory roles in regulating Rhp26 activities (Fig. 1*A* and *SI Appendix*, Fig. S1*A*) (21).

As an orphan remodeler, CSB has its own specific NTR and CTR that are significantly distinct from those in other well-characterized remodelers (5). CSB activities are inhibited by its NTR and stimulated by its CTR and NAP1-like histone chaperones (21, 26, 27), but the molecular mechanisms of chromatin remodeling and nucleosomal epitope recognition by CSB remain elusive. Several important mechanistic questions remain unclear: What is the regulatory motif that couples its ATPase activity and translocation activity for efficient chromatin remodeling? What are the nucleosomal epitopes that CSB protein recognizes for remodeling? What are the outcomes of chromatin remodeling by CSB (nucleosome eviction or sliding), and what factors control these outcomes? Is CSB distinct from other canonical remodelers in terms of remodeling mechanisms and substrate recognition? Is the CSB chromatin-remodeling activity essential and sufficient for supporting effective DNA repair? Here we investigated the molecular mechanism of chromatin remodeling by CSB by analyzing its yeast ortholog, Rhp26. We found that the remodeling mechanism and nucleosomal epitope recognition by Rhp26 are different from those of other well-studied canonical SNF2-like remodelers such as ISWI and SWI/SNF.

Results

The Side Chain of the Leucine-Latch Motif Is Critical for the Auto-Repression of Rhp26 Chromatin-Remodeling Activity. Our previous study revealed that the enzymatic activities of full-length Rhp26 (such as ATPase, DNA translocation, and chromatin-remodeling activities) are auto-repressed by its conserved leucine-latch motif (L_7xxL_{10}) at the NTR (21). We also demonstrate that mutated Rhp26 proteins, mimicking the release of this specific auto-inhibition, show robust chromatin-remodeling activities. These mutated Rhp26 proteins, with disruption of the local helical structure ($Rhp26^{7P/10P}$ or $Rhp26^{7G/10G}$) or deletion of the entire NTR region (1–205, $Rhp26^{\Delta N}$), provide important insights into understanding the molecular basis of auto-regulatory mechanisms by the leucine-latch motif (21). However, it is not clear whether the hydrophobic side chain of the conserved leucine residues or the helical structure of the leucine-latch motif is responsible for this auto-inhibition. To address this question, we generated a new leucine-latch motif mutant ($Rhp26^{7A/10A}$) with substitution of two conserved Leu residues to Ala (L7A/L10A) (*SI Appendix*, Fig. S2*A*). Unlike $Rhp26^{7P/10P}$, $Rhp26^{7A/10A}$ is expected to preserve the predicted short helix structure. In addition, we also generated a short deletion of the first 16 amino-terminal residues containing the leucine-latch ($Rhp26^{\Delta 16}$), which allows us to understand the effect of deletion of the leucine-latch motif in comparison with the whole NTR deletion $Rhp26^{\Delta N}$ (206–973). We systematically compared and characterized these two new mutants ($Rhp26^{7A/10A}$ and $Rhp26^{\Delta 16}$) and two previously reported mutants ($Rhp26^{7P/10P}$ and $Rhp26^{\Delta N}$) using two distinct chromatin-remodeling assays (Fig. 1 *B*–*E* and *SI Appendix*, Fig. S3). In a mononucleosome-remodeling assay, we found that all of these active forms of mutants disrupt mononucleosomes and generate a naked DNA band (Fig. 1 *B* and *C*). $Rhp26^{7A/10A}$ is able to stimulate Rhp26 chromatin-remodeling activity to about a half level as $Rhp26^{7P/10P}$, whereas the deletion of the leucine-latch motif alone in $Rhp26^{\Delta 16}$ greatly activates Rhp26-remodeling activity to a similar level as $Rhp26^{\Delta N}$. Similar results were obtained from restriction enzyme accessibility assays, with chromatin reconstituted onto circular plasmid DNA (which mimics the chromatin of circular minichromosomes) (Fig. 1 *D* and *E*). The disappearance of top bands and the appearance of bottom bands correlate to active chromatin-remodeling events. The levels of activation by these mutants are ranked as follows: $Rhp26^{\Delta 16} = Rhp26^{\Delta N} > Rhp26^{7P/10P} > Rhp26^{7A/10A}$ (Fig. 1 *B*–*E*). Taken together, these results confirmed the importance of the leucine-latch motif in inhibiting Rhp26 chromatin-remodeling activity. Shortening the side chain in leucine residues of the leucine-latch motif (substitution of Leu to Ala) partially releases this auto-inhibition, and deletion of the first 16 amino acids containing the leucine-latch motif is sufficient to achieve full activation of Rhp26. These Rhp26 derivatives mimic the active form of Rhp26 upon the release of Rhp26's N-terminal auto-inhibition and serve as great model proteins for studying the molecular mechanism of Rhp26 chromatin remodeling.

CSB-Specific Coupling Motif at the C-Terminal Region Is Essential for Chromatin Remodeling. Deletion of the whole C-terminal region (852–973) of Rhp26 completely abolishes its enzymatic chromatin-remodeling activity in vitro (21). Also, the *rhp26ΔC* strain is hypersensitive to UV damage in vivo, suggesting important functional roles of the CTR in chromatin remodeling and DNA repair. To further map the exact region of CTR that is responsible for supporting chromatin remodeling, we purified a variety of Rhp26 C-terminal truncations (*SI Appendix*, Fig. S2) and tested their chromatin-remodeling activities in vitro. Since the basal levels of chromatin-remodeling activities for the full-length protein are extremely low due to the auto-inhibition by its leucine-latch motif, these experiments were done in backgrounds with mutations to the leucine-latch motif (either deletions or point mutations), which release this inhibition. Intriguingly, we found that while $Rhp26^{17\text{-}910}$ is as active as $Rhp26^{\Delta 16}$ (17–973) in terms of chromatin-remodeling activity, in sharp contrast, the closely related shorter C-terminal truncation $Rhp26^{17\text{-}900}$ is completely inactive in chromatin remodeling (Fig. 2*A*). Consistently, $Rhp26^{17\text{-}910}$, but not $Rhp26^{17\text{-}900}$, is able to translocate and displace the ssDNA in the triplex displacement assay (Fig. 2*B*). Next, we investigated how these truncations affect ATPase activity. $Rhp26^{17\text{-}900}$ has a modest ATPase activity, whereas $Rhp26^{17\text{-}910}$ has a stronger ATPase activity that is comparable to that of $Rhp26^{\Delta 16}$ (17–973) (Fig. 2*C*). These results revealed that the $Rhp26^{17\text{-}900}$ mutant is able to hydrolyze ATP but fails to translocate along DNA, suggesting that the 901–910 region is important for coupling these two activities.

We further examined the sequence around the 901–910 region and found that it belongs to a three-helix cluster motif that is highly conserved within all CSB family proteins (*SI Appendix*, Fig. S1*B*), but not in other chromatin remodelers. To further investigate the roles of key residues in the region of the CSB-specific coupling motif in 901–910 (termed "region A"), we substituted the two conserved residues H902/D903 with Ala (HD/AA) and purified the mutant protein of $Rhp26^{\Delta 16\text{-HD/AA}}$. Intriguingly, the chromatin-remodeling activity of $Rhp26^{\Delta 16\text{-HD/AA}}$ is completely abolished in comparison with $Rhp26^{\Delta 16}$. In contrast, $Rhp26^{\Delta 16\text{-HD/AA}}$ still maintains reasonable ATPase activity, suggesting that the loss of remodeling of $Rhp26^{\Delta 16\text{-HD/AA}}$ is not due to incapability of ATP hydrolysis (Fig. 2*D* and *SI Appendix*, Fig. S2*C*). Our results suggest that the first two helices of the CSB-specific motif (the 879–910 region), in particular the conserved residues (H902/D903) in the 901–910 region (region A), are essential for Rhp26 chromatin remodeling and translocation activities in vitro. Therefore, we termed the region a "CSB-specific coupling motif," which is important for coupling Rhp26 ATPase activities and chromatin remodeling/translocation activities. Our in vitro results also suggest that the rest of CTR (911–973, region B) is dispensable for Rhp26 chromatin remodeling. Taken together, we revealed two regions in CTR that have distinct roles in chromatin remodeling: region A (901–910) is essential for chromatin remodeling, whereas region B (911–973) is not.

Distinct Functions of Rhp26 C-Terminal Region A and Region B in Vivo. To assess the functions of the C-terminal region of Rhp26 in vivo, we cloned these C-terminal truncation fragments into

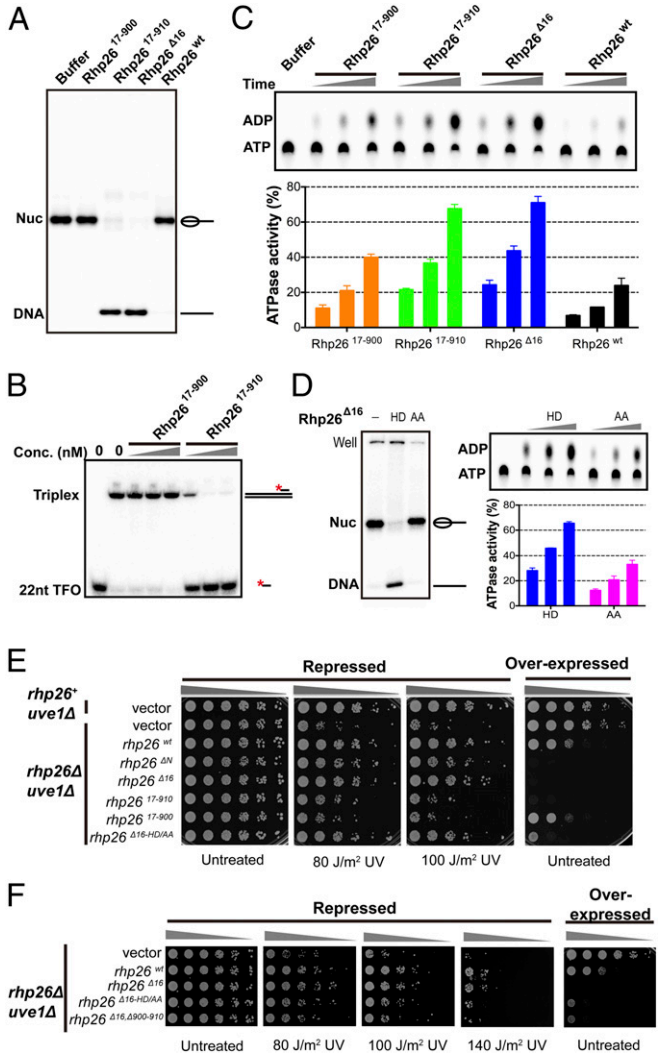

Fig. 2. The C-terminal 901–910 region is essential for Rhp26 chromatin remodeling. (*A*) The mononucleosome-remodeling assay showed that Rhp26$^{17\text{-}910}$ and Rhp26$^{\Delta 16}$ have robust remodeling activities, whereas Rhp26$^{17\text{-}900}$ and Rhp26^{wt} do not. The 2-nM (0-*N*-70) nucleosome substrate and 300-nM remodelers were incubated for 1.5 h before the reaction was quenched. (*B*) Triplex disruption assay by comparison of Rhp26$^{17\text{-}900}$ and Rhp26$^{17\text{-}910}$. The results further confirmed that the 901–910 region is key for CSB translocase activity, which is considered to be as consistent as chromatin-remodeling activity. The 22-nt TFO was labeled at 5′ ^{32}P and shown as a red asterisk. The gradient remodeler concentrations are 50, 200, and 600 nM. (*C*) DNA-dependent ATPase activity of Rhp26 and Rhp26 C-terminal truncations. In contrast to Rhp26^{wt}, Rhp26$^{17\text{-}910}$ and Rhp26$^{\Delta 16}$ have robust ATPase activities, but Rhp26$^{17\text{-}900}$ showed modest ATPase activity. The error bars are the SD based on three independent experiments. (*D*) Substitution of H902A/D903A completely abolishes the remodeling activities of Rhp26$^{\Delta 16}$. (*E*) Genetic analysis of Rhp26 mutants in *S. pombe*. Low-level expression under repressed conditions show that the C-terminal region (911–973, region B) is crucial for repair of UV-induced DNA damage. Overexpression of *rhp26* fragments proficient in chromatin-remodeling activities is toxic in *S. pombe*. (*F*) Mutation or deletion of region A partially rescues overexpression toxicity and partially hinders repair of UV-induced DNA damage.

plasmids with a thiamine-repressible *nmt41* promoter, which allowed us to test strains under two different conditions: the repressed low-level expression and overexpression conditions. These plasmids were transformed into *S. pombe* cells lacking endogenous *rhp26* and *uve1(uvde)* genes, the latter of which acts in a parallel pathway in UV excision repair. Consistent with previous results (21), low-level expression of Rhp26$^{\Delta N}$ is sufficient to rescue the UV sensitivity of *rhp26Δ uve1Δ* cells to the same level as wild-type (WT) *rhp26*$^{+}$ (Fig. 2*E*). On the other hand, overexpression of Rhp26$^{\Delta N}$ is highly toxic to cells, and colonies failed to form even in the absence of DNA damage. Rhp26$^{\Delta 16}$ phenocopies Rhp26$^{\Delta N}$ in both UV sensitivity and overexpression toxicity. These results highlight the importance of the balanced regulation of Rhp26 enzymatic activity in vivo (Fig. 2*E*).

Intriguingly, we found that truncating the C-terminal region in the Rhp26$^{\Delta 16}$ background results in the loss of UV damage resistance under repressed conditions (Fig. 2*E*), suggesting that the C terminus of Rhp26 plays a critical role in UV-induced DNA damage repair. To further dissect the contributions of region A and region B in UV survival, we first compared UV sensitivities of the following mutants: Rhp26$^{\Delta 16}$ (containing both region A and region B), Rhp26$^{17\text{-}910}$ (containing region A only), and Rhp26$^{17\text{-}900}$ (lacking both region A and region B). We ranked the strains in terms of resistance to UV damage: Rhp26$^{\Delta 16}$ (containing both region A and region B) > Rhp26$^{17\text{-}910}$ (containing region A only) ≥ Rhp26$^{17\text{-}900}$ (lacking both region A and region B) (Fig. 2*E*). These results demonstrated the important role of region B for UV survival. To further evaluate the contribution of region A mutants to UV survival in the presence of region B, we compared two additional mutants, Rhp26$^{\Delta 16/\Delta 900\text{–}910}$ (with an internal deletion of region A) and Rhp26$^{\Delta 16\text{-HD/AA}}$ (with pointed mutations in region A) with Rhp26$^{\Delta 16}$ (containing both region A and region B). We ranked the UV survival strains in the following order: Rhp26$^{\Delta 16}$ > Rhp26$^{\Delta 16\text{-HD/AA}}$ > Rhp26$^{\Delta 16/\Delta 900\text{–}910}$ (Fig. 2*F*). These results revealed the contribution of region A to UV survival. Taken together, we demonstrate that both region A and region B are required for UV survival.

We also evaluated the overexpression toxicities of different strains and found that overexpression of Rhp26$^{17\text{-}910}$ is toxic to cells, which phenocopies Rhp26$^{\Delta N}$ and Rhp26$^{\Delta 16}$. This result also suggests that region B is dispensable for this phenotype. In sharp contrast, deletion or substitution of the conserved HD residues in the 901–910 region (region A) alleviated this overexpression toxicity (as in Rhp26$^{17\text{-}900}$, Rhp26$^{\Delta 16\text{-HD/AA}}$ and Rhp26$^{\Delta 16/\Delta 900\text{–}910}$). These results revealed an intriguing correlation between overexpression toxicity in vivo and constitutively active chromatin-remodeling activities in vitro. Overexpression of all proteins with constitutively active chromatin-remodeling activities (Rhp26$^{\Delta N}$, Rhp26$^{\Delta 16}$, or Rhp26$^{17\text{-}910}$) is toxic to cells. This overexpression toxicity is likely due to uncontrolled constitutively active chromatin remodeling.

Taken together, we were able to dissect distinct functions of CTR regions. We identified that region A (901–910) is essential for active chromatin remodeling and the overexpression toxicity phenotype, whereas region B (911–973) is dispensable for these activities. In sharp contrast, we demonstrated that both region A and region B play important roles in contributing to UV damage resistance. These results underscore the important relationship between Rhp26 chromatin-remodeling activity and its role in DNA repair. The full function of Rhp26 in DNA repair requires not only region A (the chromatin-remodeling–coupled motif), but also the extended C-terminal region B, which could be involved in interaction with other repair proteins in TC-NER.

Chromatin-Remodeling Activity of Rhp26 Is Dependent on H3/H4 Tails. The functional interplay between chromatin remodelers and the epitopes that they recognize, such as histone tails and extra nucleosomal linker DNA, varies greatly between the diverse families of remodelers (5, 28–31). To better understand whether histone tails have any effects on the remodeling activity of Rhp26, we prepared a series of tailless histone nucleosomes to carry out the restriction enzyme accessibility assay with minichromosomes (32). We first compared how a global loss of histone tails would affect the remodeling activities of three remodelers: Rhp26$^{7P/10P}$,

Drosophila ISWI, and human Brg1 by using nucleosome substrates with all histone tails deleted (TL) or WT histones. We found that the chromatin-remodeling activities of these three remodelers on TL are very distinct: Rhp26$^{7P/10P}$ and ISWI are significantly reduced for TL in comparison with WT nucleosomes (Fig. 3 *A* and *B*). In contrast, the status of histone tails in nucleosomes has a very minor effect on Brg1 activities in vitro (Fig. 3*C*), the essential motor subunit of the BAF-remodeling complex, which is consistent with a previous report (28). To further dissect which histone tails are critical for Rhp26-remodeling activities, we tested the remodeling activities using nucleosomes with single and double histone tail deletions (Fig. 3 *D* and *E*). As shown in Fig. 3*D*, deletion of both H3 and H4 tails greatly reduces the remodeling activities of Rhp26$^{7P/10P}$ (lanes WT and gH3,4), whereas deletion of both H2A and H2B tails has almost no effect (lanes WT and gH2A,B). We further revealed that deletion of H4 tails alone (gH4) reduces the remodeling activities of Rhp26$^{7P/10P}$ to a similar level for the TL substrate (lanes WT, TL, and gH4). Deletion of H3 tails alone (gH3) also causes small but reproducible reduction in activity (lanes WT, TL, and gH3). In contrast, we found that the remodeling activity of ISWI is strictly regulated by histone H4 tails alone (Fig. 3*E*). Indeed, this is consistent with previous literature showing that a basic patch ("KRHRK" from the 16th to 20th amino acid) at the N terminus of the H4 tail is critical in regulating ISWI activities (6, 7, 33). To investigate whether Rhp26 could recognize the same basic patch of the H4 tail, we assembled nucleosomes with a substitution of the H4 basic patch with five Ala residues (H4^{5A}) (Fig. 3*F*). As expected, ISWI-remodeling activity was abolished by H4^{5A} substitution (Fig. 3*H*) (6, 7, 33). In sharp contrast, the same H4^{5A} substitution has only a moderate effect on Rhp26-remodeling activity (Fig. 3*G*). This result reveals that the H4 tail recognition mechanisms are different between Rhp26/CSB and ISWI.

To quantitatively evaluate the impacts of histone tails on Rhp26 remodeling, we analyzed how H3 or H4 tails influenced the kinetics of Rhp26$^{\Delta 16}$-remodeling activity using a mononucleosome assay (Fig. 4*A*) and found that the remodeling rate for a WT nucleosome is $k_{obs,WT} = 0.65 \pm 0.09$ min^{-1}. Deletion of H4 tails greatly reduces the remodeling rate by ~3.6-fold ($k_{obs,gH4} = 0.18 \pm 0.04$ min^{-1}), whereas deletion of H3 tails reduces the remodeling rate by ~1.6-fold ($k_{obs,gH3} = 0.41 \pm 0.08$ min^{-1}). This result is fully consistent with our above-mentioned result using the minichromosome remodeling assay. Another interesting phenomenon that we observed is an increase in nucleosome-repositioning bands for remodeling of the gH4 nucleosome substrate in comparison with the WT nucleosome substrate (Fig. 4*B*). We quantified the production of free DNA release and nucleosome-repositioning bands separately (Fig. 4*C*). Interestingly, we found that deletion of H4 tails (gH4) greatly reduces the production of free DNA bands and increases the production of nucleosome-repositioning bands.

Flanking DNA Is Necessary for Higher Remodeling Activity of Rhp26. Many SNF2-like remodelers preferentially interact with nucleosomes containing extranucleosomal linker DNA (34, 35). To

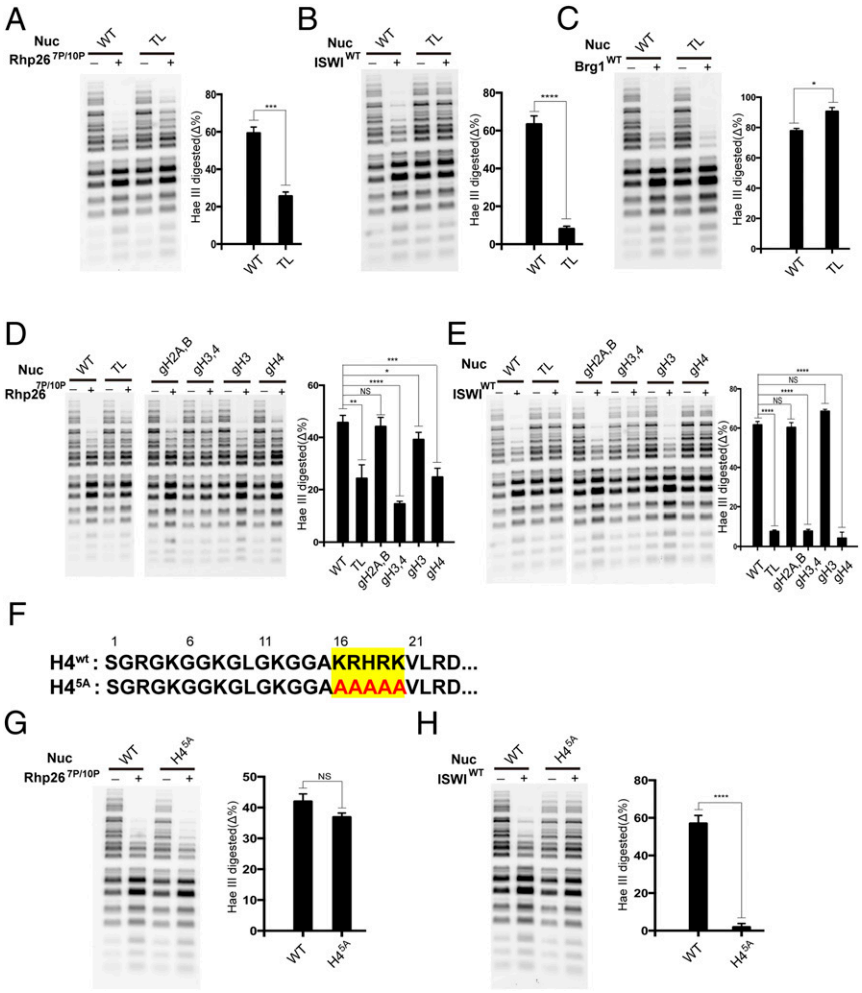

Fig. 3. The H4 tail is important for Rhp26-mediated nucleosome remodeling, revealed by a minichromosome-remodeling assay. Deletion of all TL reduced the remodeling activity of Rhp26$^{7P/10P}$(*A*) and ISWI^{WT} (*B*), but had little effect on Brg1^{WT}-mediated chromatin-remodeling activity (*C*). The effect of deletion of double-histone tails (gH2A,B and gH3,4) or single-histone tails (gH3 and gH4) on chromatin-remodeling activities by Rhp26$^{7P/10P}$ (*D*) and ISWI^{WT} (*E*), respectively, is shown. The results show that the Rhp26 chromatin-remodeling activity is related to H3 (minor) and H4 (major) tails. (*F*) The scheme of the basic patch five-alanine mutation (5A) of H4 tail. (*G*) Minichromosome-remodeling assay showed that 5A mutations of H4 tail have little effect on Rhp26$^{7P/10P}$ activity compared with WT H4. (*H*) ISWI-remodeling activity is abolished by 5A mutations of the basic patch of the H4 tail. The results reveal that Rhp26 and ISWI might adopt different H4 tail-related remodeling mechanisms. All data are displayed as mean and SD ($n = 3$). *$P < 0.05$; **$P < 0.01$; ***$P < 0.001$; ****$P < 0.0001$, two-tailed Student's *t* test.

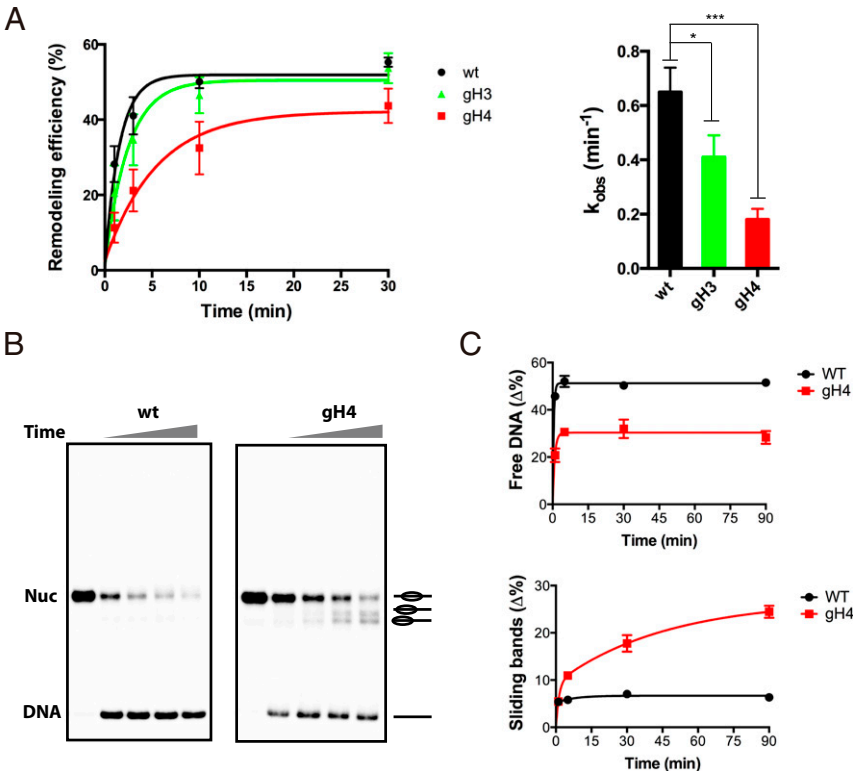

Fig. 4. The loss of H4 tail reduces Rhp26$^{\Delta 16}$-remodeling activity and changes the remodeling pattern from direct ejection to sliding using mononucleosome-remodeling assays. (*A*) Quantitative analysis of Rhp26$^{\Delta 16}$-remodeling activities with different nucleosome substrates (wt, gH3, and gH4). The concentrations of nucleosome substrates (43-*N*-39) and Rhp26$^{\Delta 16}$ are 2 and 50 nM, respectively. Reactions are quenched at 0, 1, 3, 10, and 30 min. *Right* panel shows that $k_{obs,WT}$ = 0.65 ± 0.09 min^{-1}, $k_{obs,gH3}$ = 0.41 ± 0.08 min^{-1}, and $k_{obs,gH4}$ = 0.18 ± 0.04 min^{-1} (based on three independent experiments). (*B*) The native gel showed the different remodeling patterns between WT and gH4 nucleosomes (35-*N*-35). For gH4 nucleosome-remodeling, more nucleosome position-shifted bands appeared. The concentrations of nucleosome and Rhp26$^{\Delta 16}$ were 7.5 and 100 nM, respectively. The time points are 1, 5, 30, and 90 min. (*C*) The quantitative analysis of native gel in *B* (n = 3). The *Top* illustrates the percentage of free DNA band. The *Bottom* shows the percentage of position-shift bands, separately.

investigate whether flanking DNA length affects CSB-remodeling activities, we performed mononucleosome-remodeling assays with linker DNA of different lengths. We used Rhp26$^{\Delta 16}$ for its robust remodeling activity, and similar results were obtained for other constitutively active mutants. Here we termed the nucleosome "*x*-*N*-*y*," where *N* denotes the "Widom 601" sequence bound by the histone octamer and *x* and *y* denote the length of upstream and downstream extranucleosomal linker DNA, respectively. We found that Rhp26$^{\Delta 16}$ was able to remodel the mononucleosomes even in the absence of flanking DNA. However, the efficiency of Rhp26$^{\Delta 16}$-remodeling activity is positively correlated to the flanking DNA length (Fig. 5*A*). Interestingly, in contrast to other well-studied remodelers, the flanking domains of which bind directly to linker DNA, such as the HSS domain in CHD1 (36) and ISWI (37–40), neither CTR nor NTR could bind to DNA (21).

To further investigate the potential directionality of Rhp26 remodeling, we designed and tested center-positioned (20-*N*-20) and edge-positioned nucleosomes (0-*N*-40) (Fig. 5 *B* and *C*). For the center-positioned nucleosome substrate (20-*N*-20), we detected faster shifting nucleosomal bands, indicating that a portion of the nucleosome is repositioned to the edge position. For the edge-positioned nucleosome substrate (0-*N*-40), we also observed a small portion of faster shifting bands corresponding to the far-edge–positioned nucleosomes. Taken together, we found that, while the major chromatin-remodeling product of Rhp26$^{\Delta 16}$ is free DNA, Rhp26$^{\Delta 16}$ has a preferential sliding directionality, going from middle to edge when it repositions the nucleosome in the process of remodeling.

The Mechanism of "Direct Eviction" Rather than "Continuous Sliding-Off" Explains the Histone Ejection Mode of Rhp26. The release of free DNA can be generated by at least two distinct mechanisms: direct eviction of histones from DNA (no requirement of DNA ends) or continuous sliding off the edge of linear DNA ends (41). To distinguish these possibilities for Rhp26, we employed three different strategies to block free DNA ends. First, we designed nucleosome substrates with linker DNA ends blocked by two different end-blocking strategies: the Lac repressor R3 system and the streptavidin-biotin system. Finally, to further test whether Rhp26 is able to disassemble nucleosomes from the nucleosomal array, we used a nucleosome array with a circular plasmid (42). We obtained similar results from all three systems, which are summarized below.

The Lac repressor R3 system takes advantage of the tight-binding Lac repressor mutant R3 (43). R3 protein binds specifically to the *lac* operator as a monovalent dimer, which was adopted previously to study nucleosome mobility and maintenance (44). We assembled nucleosome flanking with R3-binding sites on both sides (Fig. 6*A*). Preincubation with R3 forms the specific nuclesome-R3 complex where the nucleosome is sandwiched by R3 (lane 6, Fig. 6 *B* and *C*). If the "continuous sliding-off mode" were dominant, we would expect to capture the dominant nucleosome-R3–repositioning complex just as we observed for ISWI (lane 8, Fig. 6*C*). If the "eviction mode" were dominant, we would observe an R3-DNA complex. Indeed, we observed that the dominant remodeling product for Rhp26$^{\Delta 16}$ was the R3-DNA complex (lane 8, Fig. 6*B*), indicating that the presence of R3 cannot prevent Rhp26$^{\Delta 16}$ from removing histones and releasing free DNA. This is in sharp contrast to ISWI, where the nucleosome-R3–repositioning complex was observed (lane 8, Fig. 6*C*). This result suggests that the direct eviction model is dominant for the Rhp26 chromatin-remodeling mechanism.

The streptavidin-biotin system blocks biotin-modified linear DNA ends with monofunctional streptavidin (A1D3) (45, 46). The streptavidin-biotin complex is one of the strongest non-covalent interactions known in nature (10^{-14} M binding affinity), and biotin is very difficult to dissociate from streptavidin (45, 46). The results shown in Fig. 6 are consistent with the R3-nucleosome–remodeling assay. The main remodeling product of Rhp26$^{\Delta 16}$ was A1D3-DNA (lane 11, Fig. 6*E*), whereas the remodeling product of ISWI was repositioning the A1D3 nucleosome (lane 5, Fig. 6*F*). In this system, we also demonstrated that the interaction

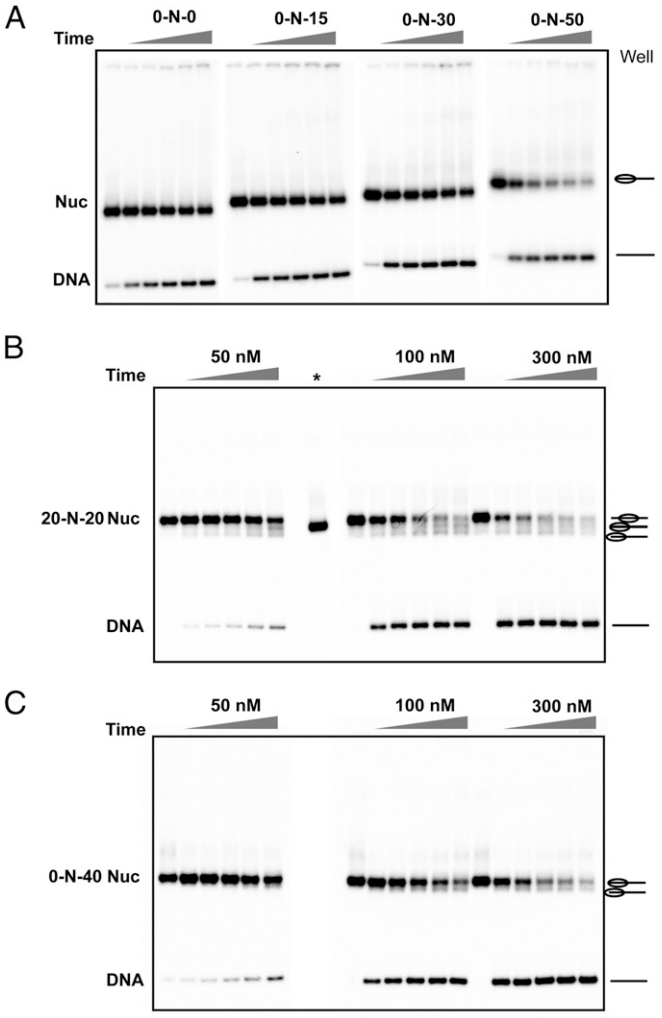

Fig. 5. The effect of extranucleosomal DNA and directionality of nucleosome remodeling by Rhp26$^{\Delta 16}$. (*A*) The effects of extranucleosomal DNA on mononucleosome-remodeling activity of Rhp26$^{\Delta 16}$. The result shows that Rhp26$^{\Delta 16}$-remodeling activity is not dependent on the extranucleosomal DNA, but its efficiency can be stimulated by longer flanking DNA. Mononucleosome-remodeling assays were performed using 300 nM Rhp26$^{\Delta 16}$ and 4 nM nucleosomes with different lengths of flanking DNA in the presence of 1 mM ATP. The time points are 0, 5, 15, 30, 60, and 90 min. (*B*) Rhp26$^{\Delta 16}$ shifts the center-positioned (20-*N*-20) mononucleosome substrate toward the edge-positioned nucleosomes and free DNA. The control lane (labeled by an asterisk) is the edge-positioned nucleosome (0-*N*-40). (*C*) Rhp26$^{\Delta 16}$ can move the edge-positioned mononucleosome (0-*N*-40) farther toward the DNA edge and generate free DNA. The final concentration of nucleosomes in the reaction is 10 nM in *B* and *C*.

between A1D3 and the DNA/nucleosome was not interrupted when excess free biotin was included. This result rules out the potential dynamic equilibrium exchange of the A1D3-biotin complex in our assays. We obtained the same result in the absence or presence of excess free biotin (lanes 11 and 12, Fig. 6*E*). This excludes the possibility that A1D3 was kicked off by the remodeler at "fast slide" mode and rebounded to naked DNA, as the A1D3 should be captured immediately by excess biotin once it has been kicked off.

To further test whether Rhp26 is able to disassemble nucleosomes from the nucleosome array, we assembled chromatin on circular DNA using a salt dialysis method and then tested Rhp26's effect on the topology of DNA supercoiling in the nucleosome (42). In the presence of ATP, but not UTP, treatment with the active form of Rhp26$^{17\text{-}910}$ and topoisomerase I (Topo I) decreased the superhelicity of nucleosomal structures on plasmid DNA in a dose-dependent manner (Fig. 6*G*; note that relaxed plasmids become positively supercoiled in chloroquine gels). These data further confirmed that Rhp26$^{17\text{-}910}$ is an ATP-dependent chromatin disassembly factor.

Based on the consistent results that we obtained from three independent systems, we conclude that Rhp26$^{\Delta 16}$ does not require free linker DNA ends for a nucleosome to slide off. Rather, it is able to release the free DNA product via direct eviction.

Discussion

Rhp26 Has a Remodeling Mechanism That Is Distinct from ISWI. Here we have elucidated the molecular basis of chromatin remodeling of Rhp26, a yeast homolog of ERCC6/CSB, and revealed that full-length Rhp26 is regulated bidirectionally via two CSB family-specific motifs. Rhp26 is auto-inhibited by its N-terminal leucine-latch motif. This CSB family-specific auto-inhibition is likely through the hydrophobic side chain of conserved leucine residues as the Leu-to-Ala mutation abolishes this auto-inhibition (Fig. 1). Furthermore, we also identified a conserved CSB family-specific coupling motif located near the C-terminal region that is essential for chromatin-remodeling activity (Fig. 7), as its removal (or substitution) completely abolishes remodeling and translocation activities but retains modest ATPase activity. This CSB-family–specific coupling motif lies outside of the core ATPase domain and does not exist in other canonical chromatin remodelers. We observed very robust remodeling activities once we removed the auto-inhibition imposed by the leucine-latch motif (k_{obs} = 0.65 min^{-1}) at a level comparable with other remodelers. In contrast, we observed a low remodeling activity of full-length Rhp26. Interestingly, previously reported remodeling activities of full-length human CSB was quite low (k_{obs} = 0.008–0.01 min^{-1}), that is, about 10- to 20-fold slower than canonical remodeling activities (ACF: 0.16 min^{-1} and SWI/SNF: 0.16 min^{-1}) (27). We speculate that this extremely low activity observed in full-length CSB is likely due to auto-inhibition by the leucine-latch motif.

Different remodelers utilize distinct recognition strategies for their nucleosomal substrates. To investigate the molecular basis of chromatin recognition by Rhp26, we compared the nucleosomal epitope requirement for Rhp26 and other canonical remodelers such as ISWI and Brg1. We found that Rhp26 has a distinct histone-tail–dependent profile, with its remodeling activity modulated by both H4 tails (major) and H3 tails (minor), whereas ISWI remodeling activity is dependent only on H4 tails. Consistent with a previous report, we observed no strong histone-tail dependence on the remodeling activity of Brg1 in vitro (28). We further revealed that the basic patch of the H4 tail is dispensable for Rhp26 activities. This is in sharp contrast to ISWI and the Chd1 family, as the same basic patch is critical for ISWI-remodeling activities (19–23, 47). Furthermore, unlike the case in ISWI that H4 tails can overcome the auto-inhibition by AutoN of ISWI, we found that the H4 tails cannot overcome the auto-inhibition imposed by the leucine-latch motif (Fig. 1). Taken together, these results suggest that Rhp26 recognizes histone tails in a distinct manner in comparison with classic remodelers such as ISWI, Chd1, and Brg1.

In addition, we also found that Rhp26 is able to remodel nucleosome core particles, suggesting that extranucleosomal DNA is not absolutely required for Rhp26 remodeling. However, the presence of extranucleosomal DNA can further stimulate the remodeling activity of Rhp26. Neither of the flanking N-terminal or C-terminal regions of Rhp26 can bind to DNA (21). This result differs from ISWI, Chd1, and Ino80, which contain additional DNA-binding domains to sense the length of extranucleosomal DNA.

One key feature of SNF2-like remodelers is that two RecA-like lobes of ATPase domains translocate along dsDNA in an ATP-dependent manner. It was proposed that the ATPase

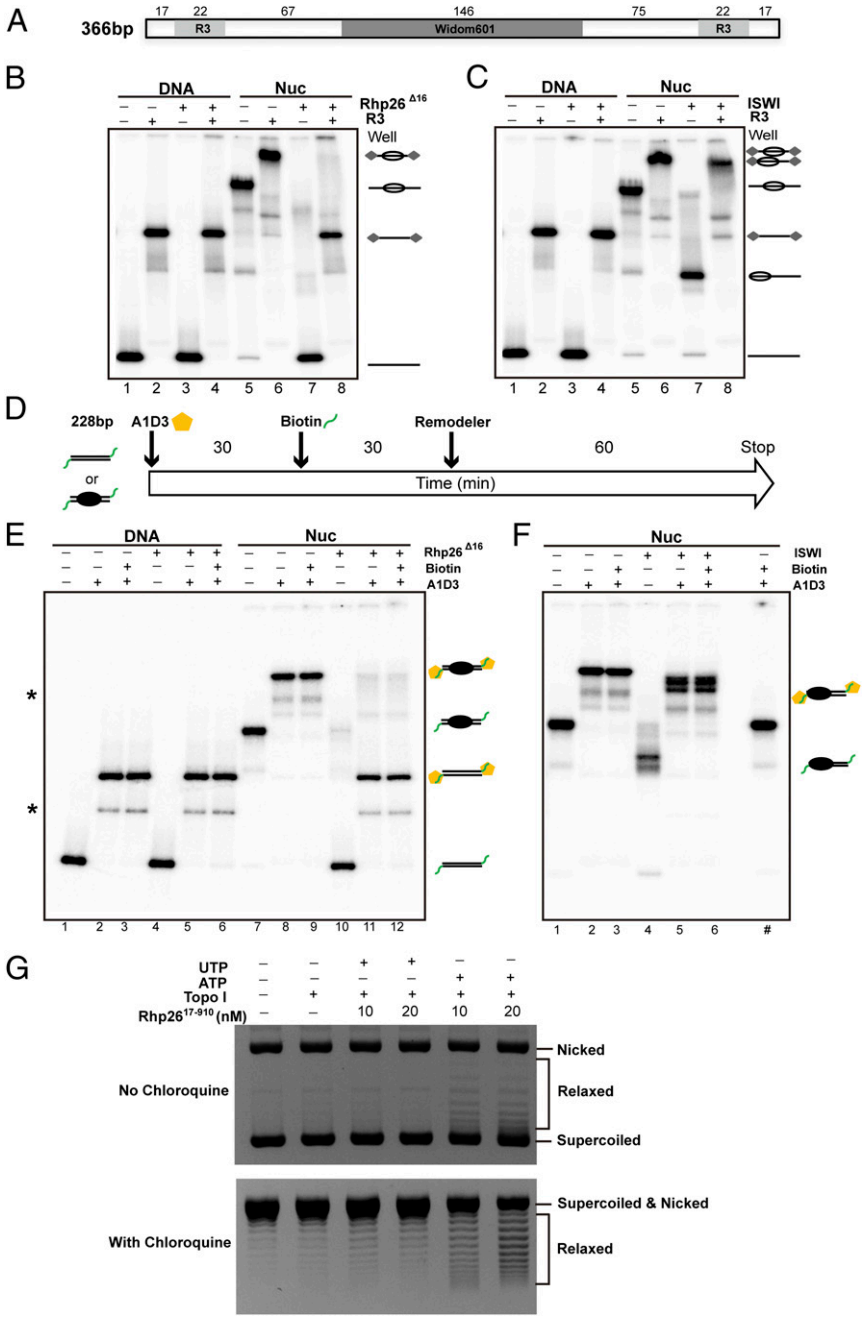

Fig. 6. Direct eviction is likely the dominant mechanism for Rhp26$^{\Delta 16}$ remodeling that results in releasing the free DNA product. (*A*) The 366-bp (106-*N*-114) DNA fragment is diagrammed as 146-bp Widom 601 in the middle and two 22-bp R3-binding sites at both ends. The remodeling assays for 2.5 nM R3-bound 366-bp DNA or nucleosome were done to interact with 300-nM Rhp26$^{\Delta 16}$ (*B*) or 10-nM ISWI (*C*) for 1 h. (*D*) Experimental timeline for the system of biotinylated 228-bp (43-*N*-39) mononucleosome blocked by streptavidin derivate A1D3 at both ends. The concentrations of DNA or nucleosome substrate, A1D3, and free biotin are 4, 100, and 10 μM, respectively. (*E*) The native gel of nucleosome remodeling for 300-nM Rhp26$^{\Delta 16}$ with 228-bp DNA or nucleosome. The minor bands labeled with an asterisk are single-biotinylated DNA or nucleosome due to PCR products (single-biotinylated dsDNA fragment) from a trace amount of unmodified primer. (*F*) The native gel of nucleosome remodeling for 5 nM ISWI with 228-bp nucleosome. The "#" lane means that the order of addition of A1D3 and biotin was reversed with incubation with 228-bp nucleosome. (*G*) Rhp26$^{17\text{-}910}$ disassembles polynucleosome arrays in the presence of ATP. Chromatin was reconstituted as nucleosome arrays using plasmid DNA and purified recombinant *Drosophila* core histones by the salt dialysis method. The reaction was carried out as indicated. Samples were deproteinized and analyzed by 0.8% agarose gel electrophoresis in the presence or absence of 10 μg/mL chloroquine. Gels were stained with ethidium bromide for visualization.

domain moves along DNA in the 3′–5′ direction (toward the nucleosome dyad). This translocation of remodelers creates DNA torsion that leads to nucleosome repositioning. Although both Rhp26 and *Drosophila* ISWI are able to move the center-positioned nucleosome toward the DNA ends, we observed that remodeling by Rhp26, but not ISWI, leads to a major portion of the free DNA product. We further showed that the free DNA product is unlikely due to continuous sliding off the free DNA ends. It was reported that high ATPase activity and strong coupling translocation activity might cause high DNA torsion that disrupts the DNA-histone contacts and results in histone ejection (Fig. 7), such as in the RSC- or SWI/SNF-remodeling complexes (41, 48).

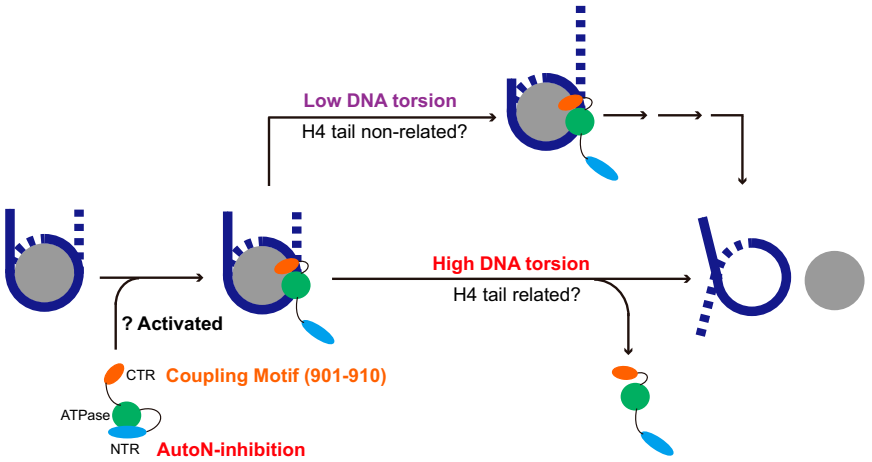

Fig. 7. Schematic model of chromatin remodeling by Rhp26. The NTR, ATPase core domain, and CTR are shown in cyan, green, and orange. The nucleosome is shown with the left wrapping of DNA (blue) around the histone octamer (gray). The proximal circle of DNA is shown as a solid line, and the distal circle is shown as a dashed line. NTR inhibits the remodeling activity of Rhp26 by the LxxL motif. Upon the release of the NTR auto-inhibition, Rhp26 is activated and binds the nucleosome. Its remodeling activity is directly dependent on the coupling motif (901–910) of CTR. There might exist two different interactions between Rhp26 and the chromatin/nucleosome. When Rhp26 translocation causes high DNA torsion, it can directly evict core histones from the nucleosome. This mode is dominant. When Rhp26 translocation causes low DNA torsion, it can just change the nucleosome position along the DNA. H4 tail plays a potential role in regulating Rhp26-remodeling patterns, which are shown in Fig. 4.

Therefore, Rhp26 behaves more like SWI/SNF or RSC than ISWI or Chd1 in terms of having a strong histone eviction tendency during remodeling.

Implications of CSB-Remodeling Activity in Chromatin Maintenance, Transcription, and DNA Repair. Nucleosomes serve as strong barriers for transcription elongation as well as DNA repair that need to be displaced during these processes. The nucleosome repositioning and removal activities observed for Rhp26 have implications in its roles in both transcription and efficient DNA repair processes. CSB is involved in chromatin remodeling and maintenance (49) and is proposed to stimulate a subset of Pol II gene expression and transcription recovery after the repair of UV damage (26, 50). Interestingly, it was reported that the recruitment of Rad26, the CSB homolog in *S. cerevisiae*, to *GAL1* gene is well correlated with a decrease of histone occupancy, although it is not clear whether it is a direct or indirect effect (51–53). Our in vitro remodeling data provide a potential direct mechanism of histone removal by *S. pombe* Rhp26.

We found a striking correlation between in vitro constitutive chromatin-remodeling activities and in vivo overexpression cellular toxicity. For all of the strains having overexpression cellular toxicity in vivo, their corresponding Rhp26 protein derivatives also have robust constitutive chromatin-remodeling activities and vice versa. For example, Rhp26$^{17\text{-}910}$ has constitutive chromatin-remodeling activities and in vivo overexpression cellular toxicity. Further truncation of the C terminus in Rhp26$^{17\text{-}900}$ leads to inactivation of chromatin-remodeling activity in vitro and rescues the overexpression toxicity in cells. In addition, elimination of the ATPase activity through the K308R mutation also showed no remodeling activity and alleviated the overexpression toxicity in cells (21). These results suggest that the overexpression toxicity observed could be the result of uncontrolled chromatin-remodeling activities. This strong correlation also highlights the importance of balanced regulation of Rhp26 chromatin remodeling and its important biological functions in cellular viability.

The relationship between CSB-remodeling activity and UV damage repair remains enigmatic. A previous study reported that a CSB-deficient cell line, CS1AN-sv, reconstituted with a chromatin-remodeling defective CSB mutant protein (hCSB$^{\Delta 245\text{–}365}$ or CSBΔN1), failed to fully rescue the UV sensitivity phenotype, suggesting the role of chromatin remodeling in supporting efficient transcription-coupled repair (27). However, since this region (245–365) is not conserved in yeast, it remains an open question regarding whether the relationship between CSB-remodeling activity and UV damage repair and survival is conserved in yeast. Are they identical, overlapped, or separate functions? Can we take advantage of a combined yeast genetic and biochemical approach to systematically dissect/map the functional domains of Rhp26 that are important for chromatin-remodeling activities and/or UV survival? Here we identify two functionally important but distinct C-terminal regions: region A (901–910) and region B (911–973). We find that the conserved region A is essential for chromatin remodeling, whereas region B is dispensable (Fig. 2*A*). In sharp contrast, in terms of resistance to UV damage, we found that both region A and region B are required (Fig. 2 *E* and *F*). Notably, we also identified specific point mutations in region A (Rhp26$^{\Delta 16\text{-HD/AA}}$) that abolish the chromatin-remodeling activity but only partially compromises survival to UV damage, suggesting that basal UV-induced DNA damage repair can be achieved presumably via region B (Fig. 2 *E* and *F*). Thus, while chromatin remodeling enacted by region A may be essential for effective DNA repair, it alone is not sufficient for supporting full UV-induced DNA damage repair. Interestingly, in human CSB, the ubiquitin-binding motif and SUMOylation site in the C-terminal region (region B) are important for UV damage repair (54, 55). However, these motifs are not conserved in yeast. How the chromatin-remodeling independent C-terminal region B in yeast CSB contributes to UV damage repair is not clear and is worthy of future mechanistic investigation. Taken together, these results suggest that the contribution of the C-terminal region of Rhp26 to UV survival can be divided into at least two parts: region A in a chromatin-remodeling–dependent manner and region B in a chromatin-remodeling–independent manner.

Bulky DNA lesions, such as UV damage, are distributed in chromatin-bound templates instead of naked DNA in vivo. Nucleosomes serve as a strong barrier for both RNA polymerases and other repair factors to access these lesions. Efficient recognition and repair of these DNA lesions requires the rearrangements or removal of nucleosomes. The chromatin-remodeling activity of CSB and other remodelers will therefore facilitate the opening of the neighboring chromatin to allow access for repair machinery assembly at DNA lesions. In addition to chromatin-remodeling–dependent

contributions, CSB also interacts with RNA Pol II as well as several DNA repair factors via protein–protein interactions (17, 18, 27, 56). These interactions, which are independent of chromatin remodeling, are also critical for efficient DNA repair.

Materials and Methods

Detailed descriptions of protein purification, DNA sequences, chromatin-remodeling assay, DNA-dependent ATPase assay, triplex disruption assay, and genetic analysis of *S. pombe* are given in *SI Appendix, Materials and Methods*.

ACKNOWLEDGMENTS. We thank Dr. Anusuya Banerjeed and Prof. Mark Howarth (University of Oxford) for the purified A1D3 streptavidin derivate.This work was supported by National Institutes of Health Grants R01 GM102362 (to D.W.), R35 GM118060 (to J.T.K.), and GM059447, CA077325, and CA117638 (to P.R.); by National Key R&D Program of China Grant 2018YFC1004500; and by National Natural Science Foundation of China Grant 31872817 (to B.L.).

1. Fairman-Williams ME, Guenther UP, Jankowsky E (2010) SF1 and SF2 helicases: Family matters. *Curr Opin Struct Biol* 20:313–324.
2. Ryan DP, Owen-Hughes T (2011) Snf2-family proteins: Chromatin remodellers for any occasion. *Curr Opin Chem Biol* 15:649–656.
3. Narlikar GJ, Sundaramoorthy R, Owen-Hughes T (2013) Mechanisms and functions of ATP-dependent chromatin-remodeling enzymes. *Cell* 154:490–503.
4. Längst G, Manelyte L (2015) Chromatin remodelers: From function to dysfunction. *Genes (Basel)* 6:299–324.
5. Clapier CR, Iwasa J, Cairns BR, Peterson CL (2017) Mechanisms of action and regulation of ATP-dependent chromatin-remodelling complexes. *Nat Rev Mol Cell Biol* 18: 407–422.
6. Clapier CR, Cairns BR (2012) Regulation of ISWI involves inhibitory modules antagonized by nucleosomal epitopes. *Nature* 492:280–284.
7. Yan L, Wang L, Tian Y, Xia X, Chen Z (2016) Structure and regulation of the chromatin remodeller ISWI. *Nature* 540:466–469.
8. Flaus A, Martin DM, Barton GJ, Owen-Hughes T (2006) Identification of multiple distinct Snf2 subfamilies with conserved structural motifs. *Nucleic Acids Res* 34: 2887–2905.
9. Hanawalt PC, Spivak G (2008) Transcription-coupled DNA repair: Two decades of progress and surprises. *Nat Rev Mol Cell Biol* 9:958–970.
10. Troelstra C, et al. (1992) ERCC6, a member of a subfamily of putative helicases, is involved in Cockayne's syndrome and preferential repair of active genes. *Cell* 71: 939–953.
11. van den Boom V, et al. (2004) DNA damage stabilizes interaction of CSB with the transcription elongation machinery. *J Cell Biol* 166:27–36.
12. Lagerwerf S, Vrouwe MG, Overmeer RM, Fousteri MI, Mullenders LH (2011) DNA damage response and transcription. *DNA Repair (Amst)* 10:743–750.
13. Yuan X, Feng W, Imhof A, Grummt I, Zhou Y (2007) Activation of RNA polymerase I transcription by Cockayne syndrome group B protein and histone methyltransferase G9a. *Mol Cell* 27:585–595.
14. Fousteri M, Vermeulen W, van Zeeland AA, Mullenders LH (2006) Cockayne syndrome A and B proteins differentially regulate recruitment of chromatin remodeling and repair factors to stalled RNA polymerase II in vivo. *Mol Cell* 23:471–482.
15. Svejstrup JQ (2002) Mechanisms of transcription-coupled DNA repair. *Nat Rev Mol Cell Biol* 3:21–29.
16. Marteijn JA, Lans H, Vermeulen W, Hoeijmakers JH (2014) Understanding nucleotide excision repair and its roles in cancer and ageing. *Nat Rev Mol Cell Biol* 15:465–481.
17. Tantin D, Kansal A, Carey M (1997) Recruitment of the putative transcription-repair coupling factor CSB/ERCC6 to RNA polymerase II elongation complexes. *Mol Cell Biol* 17:6803–6814.
18. Xu J, et al. (2017) Structural basis for the initiation of eukaryotic transcription-coupled DNA repair. *Nature* 551:653–657.
19. Licht CL, Stevnsner T, Bohr VA (2003) Cockayne syndrome group B cellular and biochemical functions. *Am J Hum Genet* 73:1217–1239.
20. Wilson BT, Lochan A, Stark Z, Sutton RE (2016) Novel missense mutations in a conserved loop between ERCC6 (CSB) helicase motifs V and VI: Insights into Cockayne syndrome. *Am J Med Genet A* 170:773–776.
21. Wang L, et al. (2014) Regulation of the Rhp26ERCC6/CSB chromatin remodeler by a novel conserved leucine latch motif. *Proc Natl Acad Sci USA* 111:18566–18571.
22. Gregory SM, Sweder KS (2001) Deletion of the CSB homolog, RAD26, yields Spt(–) strains with proficient transcription-coupled repair. *Nucleic Acids Res* 29:3080–3086.
23. Yasuhira S, Morimyo M, Yasui A (1999) Transcription dependence and the roles of two excision repair pathways for UV damage in fission yeast Schizosaccharomyces pombe. *J Biol Chem* 274:26822–26827.
24. Kanamitsu K, Ikeda S (2011) Fission yeast homologs of human XPC and CSB, rhp41 and rhp26, are involved in transcription-coupled repair of methyl methanesulfonate-induced DNA damage. *Genes Genet Syst* 86:83–91.
25. Hauk G, Bowman GD (2011) Structural insights into regulation and action of SWI2/SNF2 ATPases. *Curr Opin Struct Biol* 21:719–727.
26. Lake RJ, Geyko A, Hemashettar G, Zhao Y, Fan HY (2010) UV-induced association of the CSB remodeling protein with chromatin requires ATP-dependent relief of N-terminal autorepression. *Mol Cell* 37:235–246.
27. Cho I, Tsai PF, Lake RJ, Basheer A, Fan HY (2013) ATP-dependent chromatin remodeling by Cockayne syndrome protein B and NAP1-like histone chaperones is required for efficient transcription-coupled DNA repair. *PLoS Genet* 9:e1003407.
28. Boyer LA, et al. (2000) Functional delineation of three groups of the ATP-dependent family of chromatin remodeling enzymes. *J Biol Chem* 275:18864–18870.
29. Längst G, Becker PB (2001) Nucleosome mobilization and positioning by ISWI-containing chromatin-remodeling factors. *J Cell Sci* 114:2561–2568.
30. Zofall M, Persinger J, Bartholomew B (2004) Functional role of extranucleosomal DNA and the entry site of the nucleosome in chromatin remodeling by ISW2. *Mol Cell Biol* 24:10047–10057.
31. McKnight JN, Jenkins KR, Nodelman IM, Escobar T, Bowman GD (2011) Extranucleosomal DNA binding directs nucleosome sliding by Chd1. *Mol Cell Biol* 31: 4746–4759.
32. Alexiadis V, Lusser A, Kadonaga JT (2004) A conserved N-terminal motif in Rad54 is important for chromatin remodeling and homologous strand pairing. *J Biol Chem* 279:27824–27829.
33. Liu X, Li M, Xia X, Li X, Chen Z (2017) Mechanism of chromatin remodelling revealed by the Snf2-nucleosome structure. *Nature* 544:440–445.
34. Farnung L, Vos SM, Wigge C, Cramer P (2017) Nucleosome-Chd1 structure and implications for chromatin remodelling. *Nature* 550:539–542.
35. Yamada K, et al. (2011) Structure and mechanism of the chromatin remodelling factor ISW1a. *Nature* 472:448–453.
36. Ryan DP, Sundaramoorthy R, Martin D, Singh V, Owen-Hughes T (2011) The DNA-binding domain of the Chd1 chromatin-remodelling enzyme contains SANT and SLIDE domains. *EMBO J* 30:2596–2609.
37. Dang W, Kagalwala MN, Bartholomew B (2006) Regulation of ISW2 by concerted action of histone H4 tail and extranucleosomal DNA. *Mol Cell Biol* 26:7388–7396.
38. Grüne T, et al. (2003) Crystal structure and functional analysis of a nucleosome recognition module of the remodeling factor ISWI. *Mol Cell* 12:449–460.
39. Hota SK, et al. (2013) Nucleosome mobilization by ISW2 requires the concerted action of the ATPase and SLIDE domains. *Nat Struct Mol Biol* 20:222–229.
40. Ludwigsen J, Klinker H, Mueller-Planitz F (2013) No need for a power stroke in ISWI-mediated nucleosome sliding. *EMBO Rep* 14:1092–1097.
41. Clapier CR, et al. (2016) Regulation of DNA translocation efficiency within the chromatin remodeler RSC/Sth1 potentiates nucleosome sliding and ejection. *Mol Cell* 62: 453–461.
42. Fei J, et al. (2018) NDF, a nucleosome-destabilizing factor that facilitates transcription through nucleosomes. *Genes Dev* 32:682–694.
43. Chen J, Alberti S, Matthews KS (1994) Wild-type operator binding and altered cooperativity for inducer binding of lac repressor dimer mutant R3. *J Biol Chem* 269: 12482–12487.
44. Pazin MJ, Bhargava P, Geiduschek EP, Kadonaga JT (1997) Nucleosome mobility and the maintenance of nucleosome positioning. *Science* 276:809–812.
45. Howarth M, et al. (2006) A monovalent streptavidin with a single femtomolar biotin binding site. *Nat Methods* 3:267–273.
46. Fairhead M, Krndija D, Lowe ED, Howarth M (2014) Plug-and-play pairing via defined divalent streptavidins. *J Mol Biol* 426:199–214.
47. Hauk G, McKnight JN, Nodelman IM, Bowman GD (2010) The chromodomains of the Chd1 chromatin remodeler regulate DNA access to the ATPase motor. *Mol Cell* 39: 711–723.
48. Gutiérrez JL, Chandy M, Carrozza MJ, Workman JL (2007) Activation domains drive nucleosome eviction by SWI/SNF. *EMBO J* 26:730–740.
49. Newman JC, Bailey AD, Weiner AM (2006) Cockayne syndrome group B protein (CSB) plays a general role in chromatin maintenance and remodeling. *Proc Natl Acad Sci USA* 103:9613–9618.
50. Proietti-De-Santis L, Drané P, Egly JM (2006) Cockayne syndrome B protein regulates the transcriptional program after UV irradiation. *EMBO J* 25:1915–1923.
51. Malik S, et al. (2010) Rad26p, a transcription-coupled repair factor, is recruited to the site of DNA lesion in an elongating RNA polymerase II-dependent manner in vivo. *Nucleic Acids Res* 38:1461–1477.
52. Malik S, Bhaumik SR (2012) Rad26p, a transcription-coupled repair factor, promotes the eviction and prevents the reassociation of histone H2A-H2B dimer during transcriptional elongation in vivo. *Biochemistry* 51:5873–5875.
53. Malik S, Chaurasia P, Lahudkar S, Uprety B, Bhaumik SR (2012) Rad26p regulates the occupancy of histone H2A-H2B dimer at the active genes in vivo. *Nucleic Acids Res* 40: 3348–3363.
54. Anindya R, et al. (2010) A ubiquitin-binding domain in Cockayne syndrome B required for transcription-coupled nucleotide excision repair. *Mol Cell* 38:637–648.
55. Sin Y, Tanaka K, Saijo M (2016) The C-terminal region and SUMOylation of Cockayne syndrome group B protein play critical roles in transcription-coupled nucleotide excision repair. *J Biol Chem* 291:1387–1397.
56. Boeing S, et al. (2016) Multiomic analysis of the UV-induced DNA damage response. *Cell Rep* 15:1597–1610.